Available online at www.sciencedirect.com
ScienceDirect
European Journal of Medicinal Chemistry 43 (2008) 862–871
EUROPEAN JOURNAL OF MEDICINAL CHEMISTRY
http://www.elsevier.com/locate/ejmech

Original article

Schiff base transition metal complexes as novel inhibitors of xanthine oxidase

Zhong-Lu You [a,b], Da-Hua Shi [a], Chen Xu [a], Qiang Zhang [a], Hai-Liang Zhu [a,*]

[a] *Institute of Functional Biomolecules, State Key Laboratory of Pharmaceutical Biotechnology, Nanjing University, Nanjing 210093, People's Republic of China*
[b] *Department of Chemistry and Chemical Engineering, Liaoning Normal University, Dalian 116029, People's Republic of China*

Received 21 January 2007; received in revised form 19 May 2007; accepted 21 June 2007
Available online 10 July 2007

Abstract

Twenty transition metal complexes with Schiff bases were evaluated for their inhibitory activities on xanthine oxidase (XO), of which 11 were newly synthesized and characterized by X-ray single crystal diffraction. It was found that 9 of the 20 complexes showed potent inhibitory activities against XO near to the standard inhibitor allopurinol. The cadmium(II) complex (**8**) had the most potent inhibitory activity with the IC_{50} value of 2.16 μM. Relationships between the structures and the activities showed that the ligands and the metal ions influenced the inhibitory activities. The XO inhibition of the Schiff base metal complexes most probably resulted from their direct interactions with the enzymes ''in the whole complex form''. These results demonstrated that the Schiff base transition metal complexes could be potential selective XO inhibitors.

Keywords: Schiff base; Complexes; Crystal structures; Xanthine oxidase; Inhibitor

1. Introduction

Schiff base transition metal complexes have been of great interest for many years since they are becoming increasingly important as biochemical, analytical and antimicrobial reagents [1]. Many Schiff base transition metal complexes are reported to have anticancer and antimicrobial activities [2–4]. It was reported that some drugs have greater activity when administered as metal complexes than that as free organic compounds [5]. So, Schiff base transition metal complexes may be an untapped reservoir for drugs.

Xanthine oxidase (XO) (EC 1.1.3.22) catalyzes the hydroxylation of hypoxanthine and xanthine to yield uric acid and superoxide anions. The enzyme is responsible for the medical condition known as gout which is caused by the deposition of uric acid in the joints leading to painful inflammation. On the other hand, superoxide anions formed by the enzyme has been linked to postischaemic tissue injury and oedema [6] as well as to vascular permeability [7]. XO can also oxidize synthetic purine drugs, such as antileukaemic 6-mercaptopurine, with loss of their pharmacological properties [8]. Then, the control of the action of XO may help the therapy of some diseases. Allopurinol, a potent inhibitor of XO has been used for the therapy of gout for a long time [9]. However, considering its side effects and its inability to prevent the formation of free radicals by the enzyme [10], the screening of new XO inhibitors is required.

As a follow-up to our previous characterization of a Schiff base zinc(II) complex as XO inhibitor [11], 20 Schiff base transition metal complexes were evaluated for their inhibitory activities against XO, of which 11 were newly synthesized. The results showed that the Schiff base metal complexes could be the potential selective XO inhibitors. The structure–activity relationship was discussed.

2. Chemistry

Eleven transition metal complexes (**1**–**11**) derived from Schiff bases were obtained from cheap, eco-friendly and

* Corresponding author. Tel.: +86 25 8359 2572; fax: +86 25 8359 2672.
E-mail address: zhuhl@nju.edu.cn (H.-L. Zhu).

0223-5234/$ - see front matter © 2007 Elsevier Masson SAS. All rights reserved.
doi:10.1016/j.ejmech.2007.06.015

commercially affordable reagents. Complexes **1**–**7** were synthesized under the solvolthermal conditions. Complexes **8**–**11** were synthesized through the traditional synthetic procedures at room temperature.

3. Results and discussion

3.1. Structure description of the complexes

Figs. 1–11 are the thermal ellipsoid plots of the complexes **1**–**11** together with the atomic labeling systems. The complexes from **1** to **7** are structurally similar trinuclear compounds. Each complex consists of two M_1L units (M_1 = Ni for **1** and **7**, Mn for **2**, **4** and **5**, Co for **3** and **6**; L = SALPD for **1**, **2** and **3**, NAPTPD for **4**, **5** and **6**) connected to each other by a completely encapsulated third metal ion M_2 (M_2 = Ni for **1** and **7**, Mn for **2** and **4**, Co for **3** and **5**, Cd for **6**) which is located on a crystallographic inversion center. The cage of each central metal ion is formed by two phenolate oxygen bridges from each M_1L moiety and by two acetato functions that furthermore connect the central with the two outer metal ions resulting in an octahedral environment for M_2. The coordination configuration around each central metal ion displays only slight distortions. The coordination polyhedra around the terminal M_1 ions are slightly distorted square pyramids for **1**–**6**, whose basal planes are built by two bridging O atoms and two imine N atoms of the Schiff base ligand, and the apical positions of the terminal metal ions are occupied by the O atom of the acetate groups. While for **7**, each terminal Ni ion has a slightly distorted octahedral geometry, an oxygen atom of a methanol molecule occupying the other axial position.

The smallest repeating unit of **8** contains one $Cd(C_{12}H_{16}N_2)$ cation and two bridging thiocyanate anions. The Cd(II) ion is in an octahedral coordination environment and is six-coordinated by two N atoms of one Schiff base ligand and two S atoms of two thiocyanate anions defining the basal plane, and by two N atoms of two different but symmetry-related thiocyanate anions occupying the axial positions. In the crystal of **8**, the $Cd(C_{12}H_{16}N_2)$ cations are linked by the bridging thiocyanate anions, forming polymeric chains.

In complex **9**, the Zn(II) ion is in a tetrahedral geometry, and is four-coordinated by two N atoms of a Schiff base ligand, and by two chloride anions. The ZnN_2Cl_2 coordination forms a distorted tetrahedral geometry, with angles subtended at the Zn ion in the range 80.9(2)–115.92(7)°. The N1–Zn1–N2 bond angle of 80.9(2)° is much smaller than the ideal value of 109.5°, which is due to the strain created by the five-membered chelate ring Zn1/N1/C1/C6/N2.

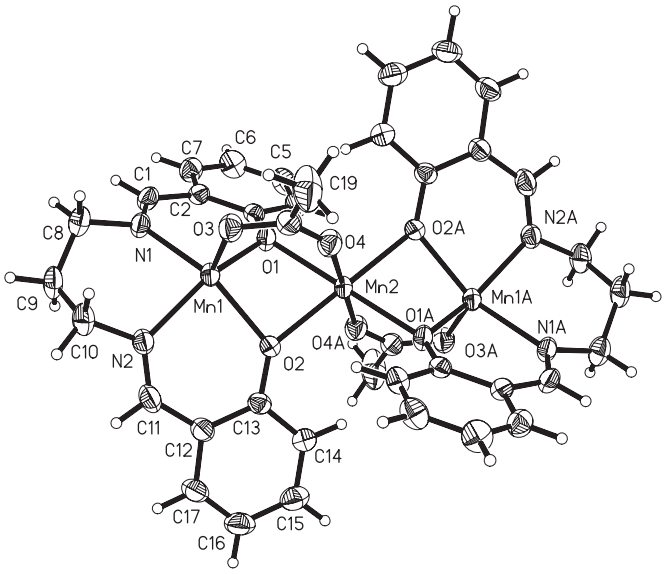

Fig. 2. Molecular structure of **2**. Displacement ellipsoids are drawn at the 30% probability level and H atoms are shown as small spheres of arbitrary radii.

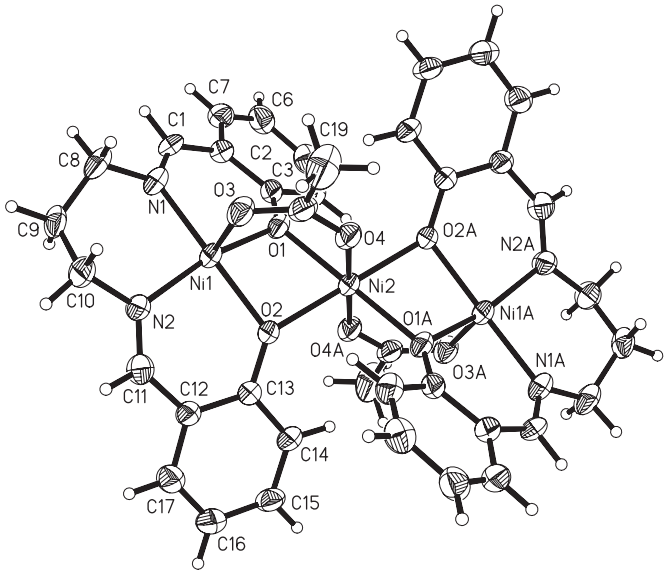

Fig. 1. Molecular structure of **1**. Displacement ellipsoids are drawn at the 30% probability level and H atoms are shown as small spheres of arbitrary radii.

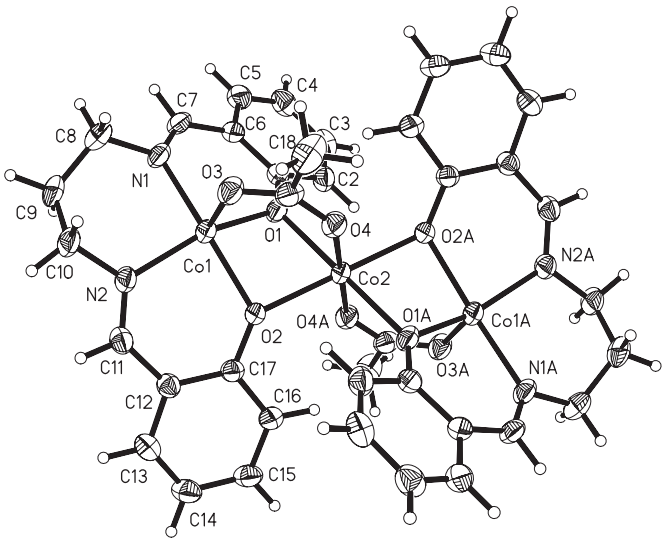

Fig. 3. Molecular structure of **3**. Displacement ellipsoids are drawn at the 30% probability level and H atoms are shown as small spheres of arbitrary radii.

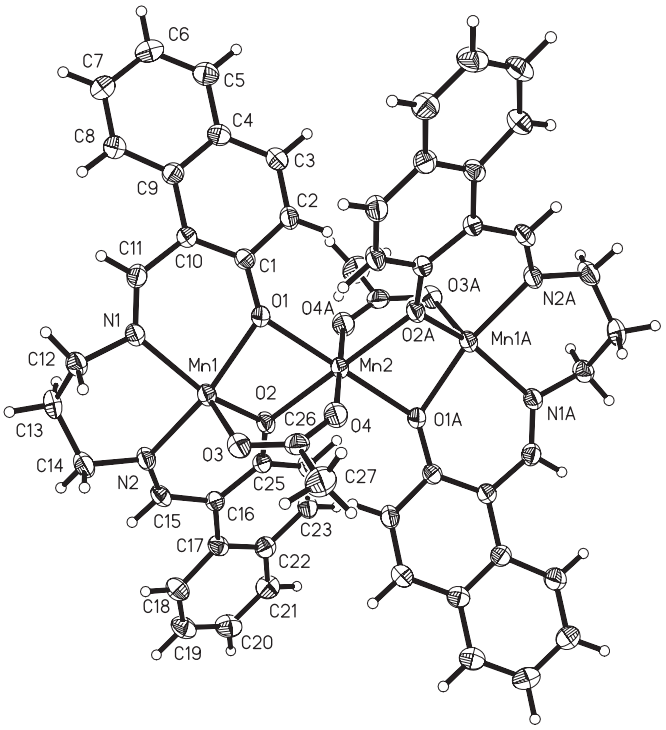

Fig. 4. Molecular structure of **4**. Displacement ellipsoids are drawn at the 30% probability level and H atoms are shown as small spheres of arbitrary radii.

The asymmetric unit of **10** contains two molecules. In both of the molecules, the Co(II) ions are in an octahedral geometry and are six-coordinated by three O and three N atoms from three Schiff base ligands.

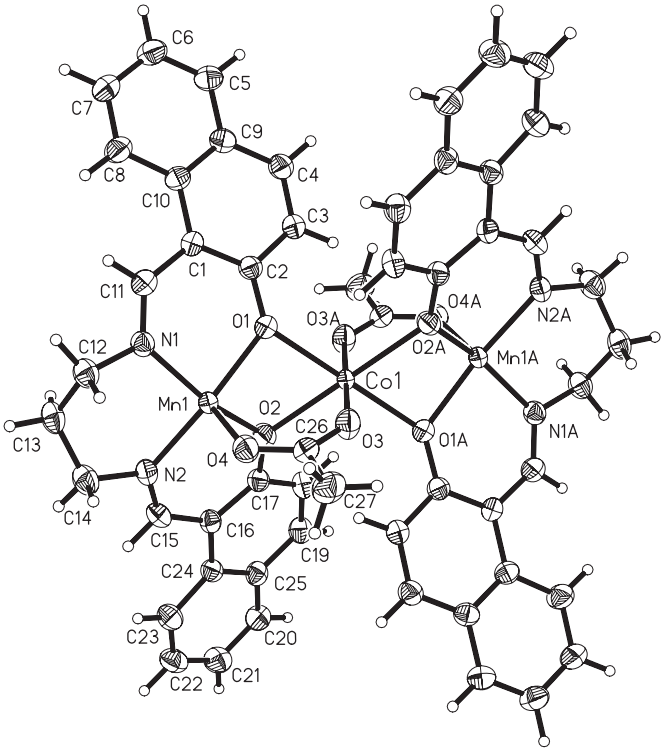

Fig. 5. Molecular structure of **5**. Displacement ellipsoids are drawn at the 30% probability level and H atoms are shown as small spheres of arbitrary radii.

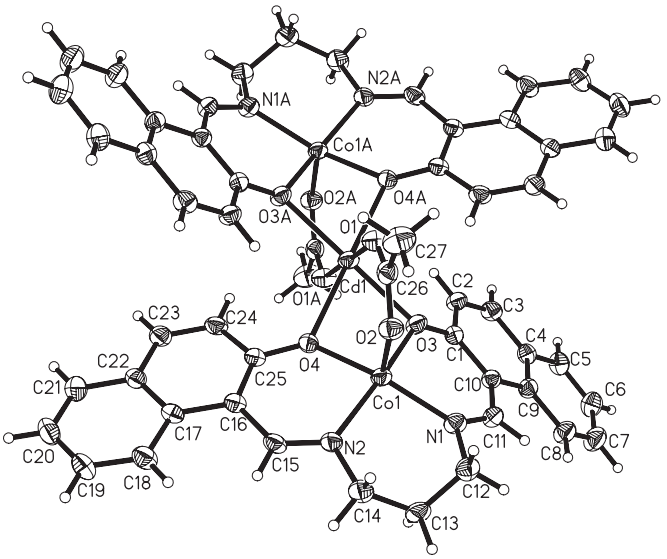

Fig. 6. Molecular structure of **6**. Displacement ellipsoids are drawn at the 30% probability level and H atoms are shown as small spheres of arbitrary radii.

Complex **11** consists of a mononuclear $[CuL(H_2O)]^+$ cation and an uncoordinated perchlorate anion. The Cu atom is in a square-planar geometry and is four-coordinated by one O and two N atoms from the Schiff base ligand, and by one O atom from the coordinated water molecule.

3.2. Inhibition of xanthine oxidase

In this study, 20 Schiff base transition metal complexes, including nickel(II), manganese(II), copper(II), cobalt(II), zinc(II) and cadmium(II) complexes, were evaluated for their inhibitory activity against XO. The results are summarized in Table 1. Among the 20 Schiff base complexes tested for XO inhibitory activities, 9 (**4**, **8**, **9**, **12**, **13**, **15**, **16**, **17** and **18**) showed

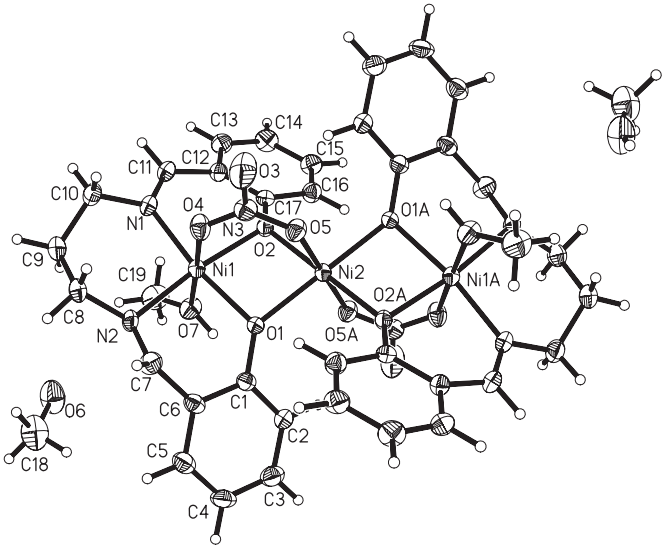

Fig. 7. Molecular structure of **7**. Displacement ellipsoids are drawn at the 30% probability level and H atoms are shown as small spheres of arbitrary radii.

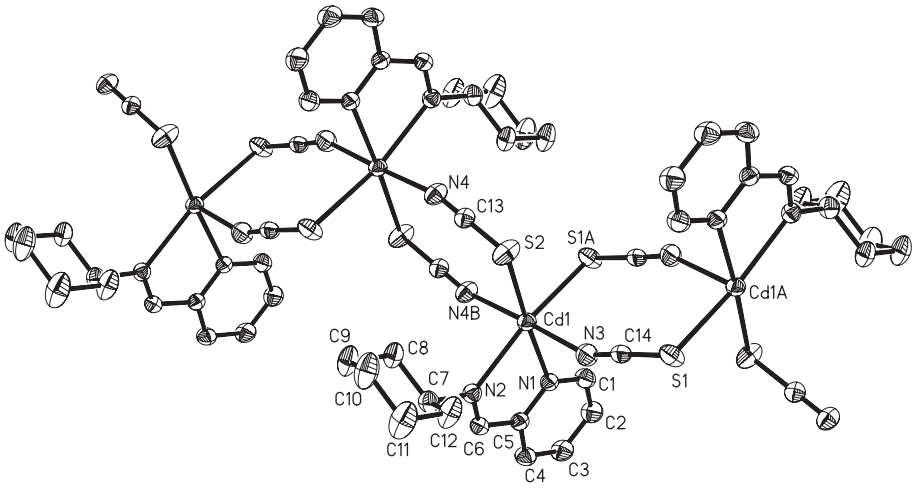

Fig. 8. Molecular structure of **8**. Displacement ellipsoids are drawn at the 30% probability level. H atoms have been omitted for clarity.

potent XO inhibitory activities near to the standard inhibitor allopurinol which had IC_{50} value of 10.30 μM. The complex **8** had the best inhibitory activity with IC_{50} value of 2.16 μM. Along with the complexes, the central metal ions involved in these complexes were also tested for the presumable XO inhibitory activities. The data was incorporated as well in Table 1. Cu(II), Cd(II) and Zn(II) possesses XO inhibitory activities with IC_{50} of 1.40, 3.67 and 46.12 μM, respectively. Ni(II), Mn(II) and Co(II) inhibit XO less than 50% at the concentration of 100 μM.

Though all of the Schiff base Cu(II) complexes had good XO inhibitory activities with IC_{50} less than 100 μM, their inhibitory activities were all lower than that of the central metal ion Cu(II). This accords to the point that Cu(II) had good inhibitory activity [12]. Schiff base Cd(II) complex **8** showed the best inhibitory action on XO with IC_{50} value of 2.16 μM. Its inhibitory activity was better than that of the central metal ion Cd(II). The XO inhibition of another Schiff base Cd(II) complexes **6** was lower than that of Cd(II). Two Zn(II) complexes possess better inhibitory activities than their central metal ions. The Schiff base Mn(II) complexes **4**, **13** and the Schiff base Co(II) complexes **15** also possess XO inhibitory activities though their central metal ions had no inhibitory activities against XO. This indicates that the XO inhibition of Schiff base metal complexes depend not only on the central ions but also on the organic ligands. Their inhibitory activities could be better or worse than their central ions. Schiff base complexes **4** and **5** had very similar structures only with the difference of M_2. Compound **4** inhibits XO with IC_{50} of 25.44 μM while the XO inhibitory activity of complex **5** was less than 50% at the concentration of 100 μM. So, the central metal ions play an important role in the XO inhibition of the Schiff base metal complexes. In summary, Schiff base metal complexes could be the inhibitors of XO and their inhibitory activities depend not only on the central mental ions but also on the ligands. It could be presumed that the discerned

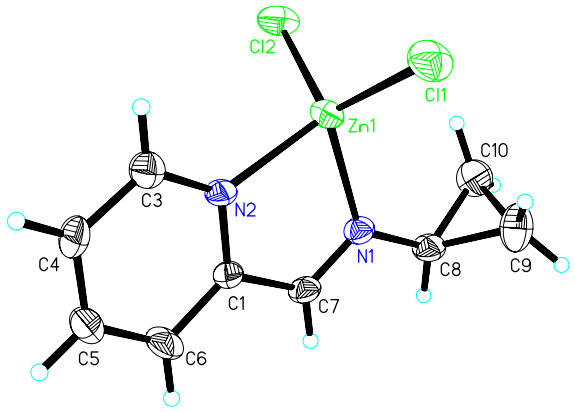

Fig. 9. Molecular structure of **9**. Displacement ellipsoids are drawn at the 30% probability level and H atoms are shown as small spheres of arbitrary radii.

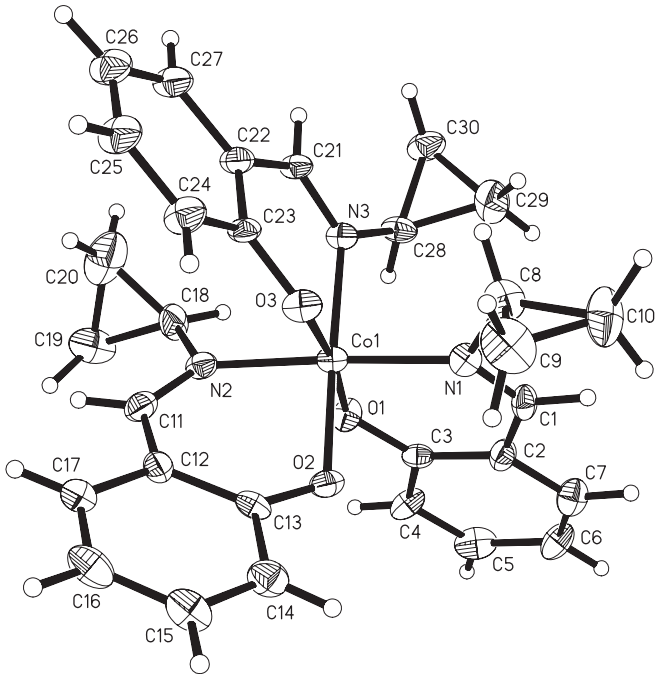

Fig. 10. Molecular structure of **10**. Displacement ellipsoids are drawn at the 30% probability level and H atoms are shown as small spheres of arbitrary radii.

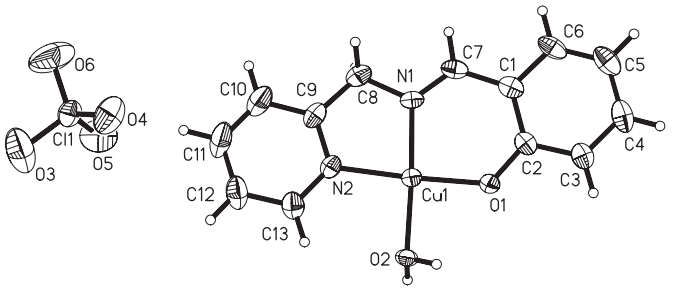

Fig. 11. Molecular structure of **11**. Displacement ellipsoids are drawn at the 30% probability level and H atoms are shown as small spheres of arbitrary radii.

inhibitions of the Schiff base metal complexes on XO most probably resulted from their direct interactions with the enzymes ''in the whole complex form'', not from the metal ions or Schiff base ligands themselves. The XO inhibition mechanisms of the Schiff base metal complexes are required to be investigated further.

Considering XO inhibitory activities of the 20 Schiff base complexes and their central metal ions, Schiff base Zn(II) and Mn(II) complexes possess better inhibitory activities than those of their central metal ions. Along with our previous work [11], Schiff base Zn(II) and Mn(II) complexes may be designed as potent XO inhibitors.

3.3. Status of *8* in aqueous solution

The UV–vis spectrum of **8** (see Fig. 12) indicates that the complex is stable at the concentration of 10^{-3} mol/L in aqueous solution. The strong absorption at 217 nm and middle absorption at 266 nm are assigned to the pyridine ring of the complex, and the absorption at 295 nm assigned to the C=N group of the ligand in the complex, all of which are more red-shifted than those of the free ligand. The weak but characteristic absorption at 406 nm is assigned to the L → M charge transfer.

The molar conductance value of the complex measured in distilled water at the concentration of 10^{-3} mol/L is 23.8 Ω^{-1} cm^2 mol^{-1}, indicating the non-electrolytic nature of the complex [13].

From the above determinations, we can conclude that complex **8** is very stable in aqueous solution.

Table 1
The inhibition of XO by the complexes and metal ions

Complexes	IC_{50} (μM)
$Ni[Ni(CH_3COO)(C_{17}H_{16}N_2O_2)]_2$	>100
$Mn[Mn(CH_3COO)(C_{17}H_{16}N_2O_2)]_2$	>100
$Co[Co(CH_3COO)(C_{17}H_{16}N_2O_2)]_2$	>100
$Mn[Mn(CH_3COO)(C_{25}H_{20}N_2O_2)]_2$	25.44
$Co[Mn(CH_3COO)(C_{25}H_{20}N_2O_2)]_2$	>100
$Cd[Co(CH_3COO)(C_{25}H_{20}N_2O_2)]_2$	>100
$Ni[Ni(ONO_2)(C_{17}H_{16}N_2O_2)(CH_3OH)]_2\cdot 2CH_3OH$	>100
$[Cd(C_{12}H_{16}N_2)(\mu\text{-}NCS)_2]$	2.16
$[Zn(C_9H_{10}N_2)(Cl)_2]$	19.47
$[Co(C_{10}H_{10}NO)_3]$	>100
$[Cu(C_{13}H_{11}N_2O)(H_2O)]\cdot ClO_4$	96.24
$Cu[Cu(CH_3COO)(C_{17}H_{16}N_2O_2)]_2$	12.99
$[Mn(C_{17}H_{16}N_2O_2)N_3]$	53.88
$[Ni(C_{16}H_{23}N_2O)_2(NCS)_2]$	>100
$[Co(C_{16}H_{23}N_2O)_2]ClO_4$	47.01
$[Cu_2(C_{16}H_{24}N_2O)_2Cl_4]$	10.38
$[Cu(C_{14}H_{22}N_2O)_2](ClO_4)_2$	23.36
$Zn[\{Zn(C_3H_4N_2)(C_{17}H_{18}N_2O_2)\}_2(NO_3)](NO_3)$	23.20
$[Cu(C_{13}H_{11}N_2O)(H_2O)](NO_3)\cdot H_2O$	81.25
$[Co(C_{20}H_{25}N_2O)_2]ClO_4$	>100
Ni(II)	>100
Mn(II)	>100
Co(II)	>100
Cu(II)	1.40
Cd(II)	3.67
Zn(II)	46.12
Allopurinol	10.34

4. Conclusion

Twenty Schiff base transition metal complexes were evaluated for their effect on XO, of which 11 were newly synthesized and characterized by X-ray diffraction. Most of the complexes showed potent inhibitory activity against XO, of which the cadmium(II) complex (**8**) was the best. The metal ions and ligands were all important for the inhibitory activities against the enzyme. The XO inhibition of the Schiff base metal complexes most probably result from their direct interactions with XO ''in the whole complex form''. Schiff base Zn(II) and Mn(II) complexes may be designed as more potent XO inhibitors by changing the ligands. Further investigation on Schiff base transition metal complexes may help to find effective XO inhibitors used in medicine and other fields with optimizing the combinations of the central metal ions and ligands.

5. Experimental protocols

5.1. Chemistry

All chemicals (reagent grade) used were commercially available. Elemental analyses for C, H and N were performed on a Perkin–Elmer 240C elemental analyzer. Complexes **12**–**20** were synthesized according to the literatures (**12**: an acetate-bridged trinuclear copper(II) complex derived from *N*,*N*′-bis(salicylidene)-1,3-propanediamine; **18**: a nitrate salt of trinuclear zinc(II) complex derived from *N*,*N*′-bis(salicylidene)-1,3-propanediamine [14]; **13**: an azide bridged one-dimensional manganese(II) complex derived from *N*,*N*′-bis (salicylidene)-1,3-propanediamine [15]; **14**: a mononuclear nickel(II) complex derived from 2-[3-(cyclohexylamino)propyliminomethyl]phenol [16]; **15**: a perchlorate salt of a cobalt(III) complex derived from 2-[3-(cyclohexylamino)propylimi nomethyl]phenol [17]; **16**: a phenolate O-bridged dinuclear copper(II) complex derived from 2-[3-(cyclohexylamino)propyliminomethyl]phenol [18]; **17**: a perchlorate salt of a mononuclear copper(II) complex derived from 2-[3-(diethylamino) propyliminomethyl]phenol [19]; **19**: a mononuclear copper(II) complex derived from 2-(pyridine-2-ylmethyliminomethyl)-phenol with a nitrate anion [20]; **20**: a perchlorate salt of a mononuclear copper(II) complex derived from 3-[(3-(cyclohexylaminopropylimino)methyl]naphthalen-2-ol [21]).

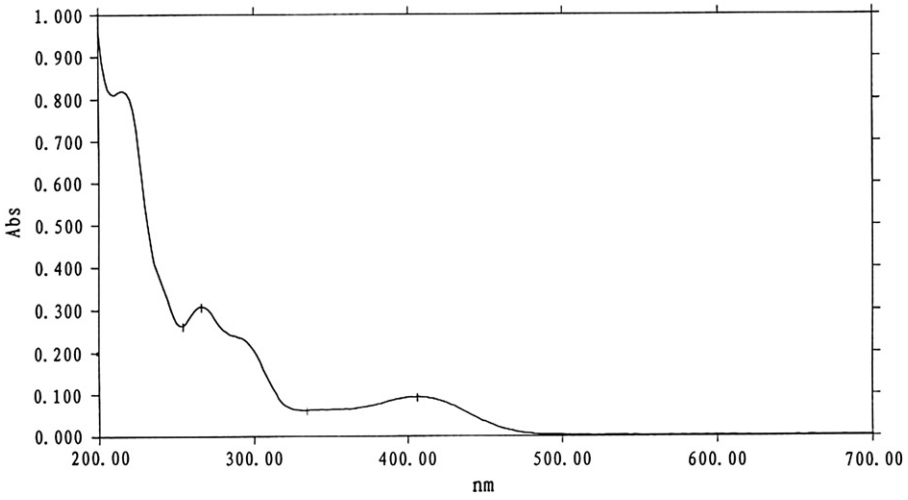

Fig. 12. UV–vis spectrum of **8**.

5.2. Preparation of the complexes

5.2.1. Ni[Ni(CH$_3$COO)(C$_{17}$H$_{16}$N$_2$O$_2$)]$_2$ (*1*)

To a MeOH solution (3 cm^3) of *N*,*N*′-bis(salicylidene)-1,3-propanediaminate (SALPD) (28.2 mg, 0.1 mmol) was added a MeOH solution (3 mL) of Ni(OAc)$_2$·4H$_2$O (24.9 mg, 0.1 mmol), with stirring for 10 min. Then the mixture was transferred to a stainless steel bomb, which was sealed, heated at 423 K for 12 h, and cooled gradually to room temperature. Green block-shaped crystals of **1** were collected, washed three times with MeOH and dried in a vacuum desiccator using anhydrous $CaCl_2$. Yield: 54.3%. Analysis: Calcd. for $C_{38}H_{38}Ni_3N_4O_8$: C, 53.4; H, 4.5; N, 6.6%. Found: C, 53.2; H, 4.6; N, 6.7%.

5.2.2. Mn[Mn(CH$_3$COO)(C$_{17}$H$_{16}$N$_2$O$_2$)]$_2$ (*2*) and Co[Co(CH$_3$COO)(C$_{17}$H$_{16}$N$_2$O$_2$)]$_2$ (*3*)

Complexes **2** and **3** were prepared by the similar procedure as described for **1**, with Ni(OAc)$_2$·4H$_2$O replaced by Mn(OAc)$_2$·2H$_2$O (20.9 mg, 0.1 mmol) and Co(OAc)$_2$·4H$_2$O

Table 2
Crystallographical and experimental data for **1**–**5**

Compound	**1**	**2**	**3**	**4**	**5**
CCDC	250089	227247	251815	256329	256331
Formula	$C_{38}H_{38}Ni_3N_4O_8$	$C_{38}H_{38}Mn_3N_4O_8$	$C_{38}H_{38}Co_3N_4O_8$	$C_{54}H_{46}Mn_3N_4O_8$	$C_{54}H_{46}CoMn_2N_4O_8$
M_r	854.85	843.54	855.51	1043.77	1047.76
T/K	298(2)	298(2)	298(2)	298(2)	298(2)
Radiation (Mo Kα), λ/Å	0.71073	0.71073	0.71073	0.71073	0.71073
Crystal shape/color	Block/green	Block/brown	Block/red	Block/brown	Block/brown
Crystal size/mm^3	0.28 × 0.25 × 0.12	0.35 × 0.30 × 0.28	0.35 × 0.28 × 0.20	0.43 × 0.35 × 0.21	0.32 × 0.28 × 0.25
Crystal system	Monoclinic	Monoclinic	Monoclinic	Monoclinic	Monoclinic
Space group	$P2_1/c$	$P2_1/c$	$P2_1/c$	$P2_1/n$	$P2_1/n$
a/Å	9.418(5)	10.554(4)	9.449(2)	11.847(5)	11.720(2)
b/Å	10.412(5)	20.716(8)	10.369(2)	11.788(3)	11.882(2)
c/Å	17.995(9)	8.408(3)	18.295(4)	16.421(4)	16.257(3)
β/°	94.513(7)	93.034(6)	94.36(3)	91.490(8)	90.66(3)
V/Å^3	1759.2(15)	1835.8(13)	1787.3(6)	2293(4)	2263.8(7)
Z	2	2	2	2	2
D_c/(g/cm^{-3})	1.614	1.526	1.590	1.512	1.537
μ/mm^{-1}	1.649	1.074	1.436	0.877	0.975
F(000)	884	866	878	1074	1078
θ range/°	2.17/25.03	2.17/25.02	2.26/25.02	2.09/25.03	2.12/25.03
Measured reflections	9102	3235	3145	4041	3984
Observed reflections $I \geq 2\sigma(I)$	1927	2379	2436	2792	2437
Absorption correction	Multi-scan	Multi-scan	Multi-scan	Multi-scan	Multi-scan
T_{min}/T_{max}	0.655/0.827	0.705/0.753	0.628/0.758	0.704/0.837	0.746/0.793
Data/restraints/parameters	3109/0/241	3235/0/241	3145/0/241	4041/0/313	3984/0/313
Goodness-of-fit on F^2	0.935	0.970	1.052	0.943	0.902
R_1, wR_2 $[I \geq 2\sigma(I)]$[a]	0.045, 0.097	0.036, 0.090	0.039, 0.102	0.035, 0.079	0.049, 0.110
R_1, wR_2 (all data)[a]	0.083, 0.107	0.055, 0.097	0.054, 0.108	0.058, 0.086	0.086, 0.123

[a] $R_1 = \sum||F_o|-|F_c||/\sum|F_o|$, $wR_2 = [\sum w(F_o^2-F_c^2)^2/\sum w(F_o^2)^2]^{1/2}$.

Table 3
Crystallographical and experimental data for **6**–**11**

Compound	**6**	**7**	**8**	**9**	**10**	**11**
CCDC	257646	250090	270827	270826	231112	244242
Formula	$C_{54}H_{46}Cd\ Co_2N_4O_8$	$C_{38}H_{48}Ni_3N_6O_{14}$	$C_{28}H_{32}Cd_2N_8S_4$	$C_9H_{10}Cl\ N_2Zn$	$C_{30}H_{30}CoN_3O_3$	$C_{13}H_{13}Cl\ CuN_2O_6$
M_r	1109.21	988.95	833.66	282.46	539.50	392.24
T/K	298(2)	298(2)	298(2)	298(2)	298(2)	298(2)
Radiation (Mo Kα), λ/Å	0.71073	0.71073	0.71073	0.71073	0.71073	0.71073
Shape/color	Block/red	Block/green	Block/colorless	Block/yellow	Block/brown	Block/blue
Crystal size/mm^3	0.42 × 0.31 × 0.15	0.28 × 0.17 × 0.12	0.32 × 0.28 × 0.25	0.35 × 0.12 × 0.12	0.43 × 0.14 × 0.06	0.23 × 0.20 × 0.18
Crystal system	Monoclinic	Triclinic	Triclinic	Triclinic	Orthorhombic	Orthorhombic
Space group	$P2_1/n$	P-1	P-1	P-1	*Pbcn*	*Pbca*
a/Å	11.772(3)	10.344(2)	9.061(2)	7.694(2)	19.330(8)	8.558(2)
b/Å	12.059(4)	10.355(2)	10.330(2)	8.725(2)	15.046(6)	15.595(2)
c/Å	16.45(2)	11.134(2)	11.072(2)	8.962(2)	36.485(15)	22.556(2)
α/°		81.97(3)	113.80(3)	98.69(3)		
β/°	90.00(2)	78.72(3)	109.17(3)	99.18(3)		
γ/°		65.30(3)	98.43(3)	91.19(3)		
V/Å^3	2335(5)	1060.3(3)	847.7(3)	586.5(2)	10611(7)	3010.3(3)
Z	2	1	1	2	16	8
D_c/(g/cm^{-3})	1.578	1.549	1.633	1.600	1.351	1.731
μ/mm^{-1}	1.215	1.391	1.532	2.512	0.683	1.661
F(000)	1128	514	416	284	4512	1592
θ range/°	2.09/25.02	1.87/25.02	2.22/27.50	2.33/27.47	2.05/25.03	2.76/27.00
Measured reflections	4112	3716	3822	1109	9217	3176
Observed reflections $I \geq 2\sigma(I)$	2960	2487	3564	1086	3146	2781
Absorption correction	Multi-scan	Multi-scan	Multi-scan	Multi-scan	Multi-scan	Multi-scan
T_{min}/T_{max}	0.629/0.839	0.697/0.851	0.640/0.701	0.474/0.753	0.758/0.960	0.701/0.754
Data/restraints/parameters	4112/0/313	3716/0/277	3822/0/190	1109/0/127	9217/0/667	3176/0/216
Goodness-of-fit on F^2	0.992	0.949	0.744	1.243	0.798	1.367
R_1, wR_2 $[I \geq 2\sigma(I)]$[a]	0.036, 0.094	0.047, 0.112	0.023, 0.063	0.033, 0.091	0.064, 0.115	0.103, 0.199
R_1, wR_2 (all data)[a]	0.057, 0.103	0.077, 0.135	0.025, 0.065	0.033, 0.091	0.205, 0.149	0.115, 0.205

[a] $R_1 = \sum||F_o|-|F_c||/\sum|F_o|$, $wR_2 = [\sum w(F_o^2-F_c^2)^2/\sum w(F_o^2)^2]^{1/2}$.

Table 4
Selected bond lengths/Å and angles/° for **1–11**

1			
Ni1–O1	1.991(3)	Ni1–O2	1.997(3)
Ni1–O3	1.983(3)	Ni1–N1	2.016(4)
Ni1–N2	1.997(4)	Ni2–O1	2.071(3)
Ni2–O2	2.035(3)	Ni2–O4	2.051(3)
O3–Ni1–O1	99.2(1)	O3–Ni1–O2	98.1(1)
O1–Ni1–O2	80.8(1)	O3–Ni1–N2	95.7(2)
O1–Ni1–N2	163.4(2)	O2–Ni1–N2	90.1(1)
O3–Ni1–N1	93.7(2)	O1–Ni1–N1	90.2(2)
O2–Ni1–N1	166.1(2)	N2–Ni1–N1	96.0(2)
O2–Ni2–O1	78.0(1)	O2–Ni2–O4	88.2(1)
O4–Ni2–O1	89.7(1)		
2			
Mn1–O1	2.092(2)	Mn1–O2	2.103(2)
Mn1–O3	2.062(2)	Mn1–N1	2.173(3)
Mn1–N2	2.154(3)	Mn2–O1	2.213(2)
Mn2–O2	2.196(2)	Mn2–O4	2.193(2)
O3–Mn1–O1	104.2(1)	O3–Mn1–O2	106.8(1)
O1–Mn1–O2	82.5(1)	O3–Mn1–N2	105.3(1)
O1–Mn1–N2	150.3(1)	O2–Mn1–N2	85.8(1)
O3–Mn1–N1	106.4(1)	O1–Mn1–N1	86.7(1)
O2–Mn1–N1	146.6(1)	N2–Mn1–N1	88.3(1)
O2–Mn2–O1	77.67(7)	O4–Mn2–O2	85.51(8)
O4–Mn2–O1	86.10(8)		
3			
Co1–O1	1.991(2)	Co1–O2	2.045(2)
Co1–O3	1.996(3)	Co1–N1	2.062(3)
Co1–N2	2.029(3)	Co2–O1	2.140(2)
Co2–O2	2.063(2)	Co2–O4	2.091(3)
O1–Co1–O3	102.4(1)	O1–Co1–N2	155.8(1)
O3–Co1–N2	100.8(1)	O1–Co1–O2	80.9(1)
O3–Co1–O2	99.6(1)	N2–Co1–O2	88.7(1)
O1–Co1–N1	89.3(1)	O3–Co1–N1	96.2(1)
N2–Co1–N1	94.9(1)	O2–Co1–N1	162.8(1)
O2–Co2–O1	77.0(1)	O2–Co2–O4	87.6(1)
O4–Co2–O1	89.9(1)		
4			
Mn1–O1	2.111(2)	Mn1–O2	2.088(2)
Mn1–O3	2.081(3)	Mn1–N1	2.126(3)
Mn1–N2	2.160(3)	Mn2–O1	2.197(2)
Mn2–O2	2.227(2)	Mn2–O4	2.156(3)
O3–Mn1–O2	100.4(1)	O3–Mn1–O1	104.9(1)
O2–Mn1–O1	82.6(1)	O3–Mn1–N1	110.6(1)
O2–Mn1–N1	148.6(1)	O1–Mn1–N1	85.0(1)
O3–Mn1–N2	100.6(1)	O2–Mn1–N2	85.5(1)
O1–Mn1–N2	153.4(1)	N1–Mn1–N2	93.1(1)
O1–Mn2–O2	77.6(1)	O4–Mn2–O1	87.0(1)
O4–Mn2–O2	89.9(1)		
5			
Co1–O1	2.177(3)	Co1–O2	2.230(3)
Co1–O3	2.176(3)	Mn1–O1	2.048(3)
Mn1–O2	2.005(3)	Mn1–O4	2.026(3)
Mn1–N1	2.028(4)	Mn1–N2	2.059(3)
O3–Co1–O1	86.4(1)	O3–Co1–O2	90.0(1)
O1–Co1–O2	74.6(1)	O2–Mn1–O4	99.1(1)
O2–Mn1–N1	157.2(1)	O4–Mn1–N1	102.8(1)
O2–Mn1–O1	82.5(1)	O4–Mn1–O1	101.2(1)
N1–Mn1–O1	87.0(1)	O2–Mn1–N2	88.3(1)
O4–Mn1–N2	95.2(1)	N1–Mn1–N2	96.1(1)
O1–Mn1–N2	162.2(1)		
6			
Cd1–O1	2.267(4)	Cd1–O3	2.260(4)
Cd1–O4	2.304(4)	Co1–O2	2.040(4)
Co1–O3	2.068(4)	Co1–O4	2.032(3)
Co1–N1	2.045(4)	Co1–N2	2.070(4)
O3–Cd1–O1	85.6(1)	O3–Cd1–O4	73.0(1)
O4–Co1–N1	155.4(1)	O1–Cd1–O4	89.7(1)
O4–Co1–O3	82.9(1)	O4–Co1–O2	100.0(1)
N1–Co1–O3	86.4(1)	O2–Co1–N1	103.8(1)
O2-Co1–N2	94.7(1)	O2–Co1–O3	101.4(1)
O3–Co1–N2	162.5(1)	O4–Co1–N2	87.7(1)
N1–Co1–N2	96.4(1)		
7			
Ni1–O1	2.003(3)	Ni1–O2	2.007(3)
Ni1–O4	2.148(4)	Ni1–O7	2.119(3)
Ni1–N1	2.002(4)	Ni1–N2	2.076(4)
Ni2–O1	2.023(3)	Ni2–O2	2.025(3)
Ni2–O5	2.122(3)		
N1–Ni1–O2	90.8(1)	N1–Ni1–N2	96.3(2)
O2–Ni1–N2	172.9(1)	O1–Ni1–O2	80.7(1)
N1–Ni1–O1	171.3(1)	O1–Ni1–N2	92.2(1)
O1–Ni1–O7	89.3(1)	N1–Ni1–O7	92.5(2)
N2–Ni1–O7	87.6(2)	O2–Ni1–O7	92.8(1)
O1–Ni1–O4	90.8(1)	N1–Ni1–O4	87.8(2)
N2–Ni1–O4	90.0(2)	O2–Ni1–O4	89.7(1)
O1–Ni2–O2	79.8(1)	O7–Ni1–O4	177.5(1)
O1–Ni2–O5	89.4(1)	O2–Ni2–O5	87.9(1)
8			
Cd1–N1	2.371(2)	Cd1–N2	2.380(2)
Cd1–N3	2.324(2)	Cd1–N4B	2.344(2)
Cd1–S2	2.646(2)	Cd1–S1A	2.722(2)
N3–Cd1–N4B	177.5(1)	N3–Cd1–N1	91.2(1)
N4B–Cd1–N1	89.3(1)	N3–Cd1–N2	92.7(1)
N4B–Cd1–N2	85.1(1)	N1–Cd1–N2	71.0(1)
N3–Cd1–S2	84.7(1)	N4B–Cd1–S2	94.896(1)
N1–Cd1–S2	175.8(1)	N2–Cd1–S2	110.1(1)
N3–Cd1–S1A	96.6(1)	N4B–Cd1–S1A	85.8(1)
N1–Cd1–S1A	88.0(1)	N2–Cd1–S1A	157.2(1)
S2–Cd1–S1A	91.5(1)		
9			
Zn1–N1	2.067(5)	Zn1–N2	2.073(4)
Zn1–Cl1	2.200(2)	Zn1–Cl2	2.210(2)
N1–Zn1–N2	80.9(2)	N1–Zn1–Cl1	114.4(1)
N2–Zn1–Cl1	115.6(1)	N1–Zn1–Cl2	114.8(1)
N2–Zn1–Cl2	110.4(1)	Cl1–Zn1–Cl2	115.9(1)
10			
Co1–O1	1.904(4)	Co1–O2	1.925(4)
Co1–O3	1.906(4)	Co1–N1	1.927(5)
Co1–N2	1.943(5)	Co1–N3	1.963(5)
Co2–O4	1.909(4)	Co2–O5	1.880(4)
Co2–O6	1.871(4)	Co2–N4	1.959(5)
Co2–N5	1.957(5)	Co2–N6	1.948(5)
O1–Co1–O3	173.4(2)	O1–Co1–O2	89.7(2)
O3–Co1–O2	87.0(2)	O1–Co1–N1	93.9(2)
O3–Co1–N1	91.6(2)	O2–Co1–N1	87.1(2)
O1–Co1–N2	84.6(2)	O3–Co1–N2	89.7(2)
O2–Co1–N2	90.6(2)	N1–Co1–N2	177.3(2)
O1–Co1–N3	93.2(2)	O3–Co1–N3	90.3(2)
O2–Co1–N3	176.3(2)	N1–Co1–N3	90.5(2)
N2–Co1–N3	91.8(2)	O6–Co2–O5	86.9(2)
O6–Co2–O4	173.2(2)	O5–Co2–O4	88.8(2)
O6–Co2–N6	91.6(2)	O5–Co2–N6	177.0(2)
O4–Co2–N6	93.0(2)	O6–Co2–N5	89.2(2)
O5–Co2–N5	90.1(2)	O4–Co2–N5	85.6(2)
N6–Co2–N5	92.5(2)	O6–Co2–N4	90.7(2)
O5–Co2–N4	86.7(2)	O4–Co2–N4	94.2(2)
N6–Co2–N4	90.8(2)	N5–Co2–N4	176.8(2)

(*continued on next page*)

Table 4 (*continued*)

11			
Cu1–O1	1.901(4)	Cu1–N1	1.921(5)
Cu1–N2	1.981(5)	Cu1–O2	1.982(4)
O1–Cu1–N1	94.0(2)	O1–Cu1–N2	174.7(2)
N1–Cu1–N2	83.5(2)	O1–Cu1–O2	89.2(2)
N1–Cu1–O2	174.9(2)	N2–Cu1–O2	92.9(2)

(24.9 mg, 0.1 mmol) for **2** and **3**, respectively. Brown block-shaped crystals of **2** and red block-shaped crystals of **3** were obtained. Yield: 81.2% for **2** and 73.7% for **3**. Analysis: Calcd. for $C_{38}H_{38}Mn_3N_4O_8$: C, 54.1; H, 4.5; N, 6.6%. Found: C, 53.9; H, 4.5; N, 6.5%; $C_{38}H_{38}Co_3N_4O_8$: C, 53.3; H, 4.5; N, 6.5%. Found: C, 53.5; H, 4.4; N, 6.7%.

5.2.3. $Mn[Mn(CH_3COO)(C_{25}H_{20}N_2O_2)]_2$ (**4**)

The complex **4** was prepared by the similar procedure as described for **2**, with SALPD replaced by NAPTPD (38.2 mg, 0.1 mmol) (NAPT PD = *N*,*N*′-bis(2-hydroxynaphthylmethenylimino)-1,3-propanediaminate). Brown block-shaped crystals of **4** were obtained. Yield: 69.3%. Analysis: Calcd. for $C_{54}H_{46}Mn_3N_4O_8$: C, 62.1; H, 4.4; N, 5.4%. Found: C, 62.0; H, 4.5; N, 5.5%.

5.2.4. $Co[Mn(CH_3COO)(C_{25}H_{20}N_2O_2)]_2$ (**5**)

To a MeOH solution (3 mL) of NAPTPD (38.2 mg, 0.1 mmol) was added a MeOH solution (3 mL) of $Mn(OAc)_2\cdot 2H_2O$ (20.9 mg, 0.1 mmol) and $Co(OAc)_2\cdot 4H_2O$ (24.9 mg, 0.1 mmol), with stirring for 10 min. Then the mixture was transferred to a stainless steel bomb, which was sealed, heated at 423 K for 12 h, and cooled gradually to room temperature. Brown block-shaped crystals of **5** were collected, washed three times with MeOH and dried in a vacuum desiccator using anhydrous $CaCl_2$. Yield: 77.2%. Analysis: Calcd. for $C_{54}H_{46}CoMn_2N_4O_8$: C, 61.9; H, 4.4; N, 5.3%. Found: C, 62.0; H, 4.5; N, 5.5%.

5.2.5. $Cd[Co(CH_3COO)(C_{25}H_{20}N_2O_2)]_2$ (**6**)

The complex **6** was prepared by the similar procedure as described for **5**, with $Mn(OAc)_2\cdot 2H_2O$ replaced by $Cd(OAc)_2\cdot 2H_2O$ (26.6 mg, 0.1 mmol). Red block-shaped crystals of **6** were obtained. Yield: 67.2%. Analysis: Calcd. for $C_{54}H_{46}CdCo_2N_4O_8$: C, 58.5; H, 4.2; N, 5.1%. Found: C, 58.3; H, 4.3; N, 4.9%.

5.2.6. $Ni[Ni(ONO_2)(C_{17}H_{16}N_2O_2)(CH_3OH)]_2\cdot 2CH_3OH$ (**7**)

The complex **7** was prepared by the similar procedure as described for **1**, with $Ni(OAc)_2\cdot 4H_2O$ replaced by $Ni(NO_3)_2\cdot 6H_2O$ (29.1 mg, 0.1 mmol). Green block-shaped crystals of **7** were obtained. Yield: 54.5%. Analysis: Calcd. for $C_{38}H_{48}Ni_3N_6O_{14}$: C, 46.2; H, 4.9; N, 8.5%. Found: C, 46.0; H, 5.1; N, 8.7%.

5.2.7. $[Cd(C_{12}H_{16}N_2)(\mu\text{-}NCS)_2]$ (**8**)

Pyridine-2-carboxaldehyde (10.7 mg, 0.1 mmol) and cyclohexylamine (9.9 mg, 0.1 mmol) were dissolved in MeOH (8 mL). The mixture was stirred for 10 min to give a yellow solution, which was added to a stirred aqueous solution (3 mL) of NH_4NCS (7.6 mg, 0.1 mmol) and a MeOH solution (3 mL) of $Cd(NO_3)_2\cdot 4H_2O$ (30.8 mg, 0.1 mmol). The mixture was stirred for another 10 min at room temperature and then filtered. The filtrate was kept in air for 7 days, forming colorless block-shaped crystals of **8**. The crystals were isolated, washed three times with MeOH and dried in a vacuum desiccator containing anhydrous $CaCl_2$. Yield: 77.1%. Analysis: Calcd. for $C_{28}H_{32}Cd_2N_8S_4$: C, 40.3; H, 3.9; N, 13.4%. Found: C, 40.5; H, 4.1; N, 13.3%.

5.2.8. $[Zn(C_9H_{10}N_2)(Cl)_2]$ (**9**)

Pyridine-2-carboxaldehyde (10.7 mg, 0.1 mmol) and cyclopropylamine (5.7 mg, 0.1 mmol) were dissolved in MeOH (8 mL). The mixture was stirred for 10 min to give a yellow solution, which was added to a stirred MeOH solution (3 mL) of $ZnCl_2\cdot 6H_2O$ (24.4 mg, 0.1 mmol). The mixture was stirred for another 10 min at room temperature and then filtered. The filtrate was kept in air for 5 days, forming yellow block-shaped crystals of **9**. The crystals were isolated, washed three times with MeOH and dried in a vacuum desiccator containing anhydrous $CaCl_2$. Yield: 45.1%. Analysis: Calcd. for $C_9H_{10}Cl_2N_2Zn$: C, 38.3; H, 3.6; N, 9.9%. Found: C, 38.0; H, 3.4; N, 10.0%.

5.2.9. $[Co(C_{10}H_{10}NO)_3]$ (**10**)

Salicylaldehyde (12.1 mg, 0.1 mmol) and cyclopropylamine (5.7 mg, 0.1 mmol) were dissolved in MeOH (8 mL). The mixture was stirred for 10 min to give a yellow solution, which was added to a stirred MeOH solution (5 mL) of $Co(OAc)_2\cdot 4H_2O$ (24.9 mg, 0.1 mmol). The mixture was stirred for another 10 min at room temperature and then filtered. The filtrate was kept in air for 7 days, forming brown block-shaped crystals of **10**. The crystals were isolated, washed three times with MeOH and dried in a vacuum desiccator containing anhydrous $CaCl_2$. Yield: 83.3%. Analysis: Calcd. for $C_{30}H_{30}CoN_3O_3$: C, 66.8; H, 5.6; N, 7.8%. Found: C, 66.6; H, 5.7; N, 7.7%.

5.2.10. $[Cu(C_{13}H_{11}N_2O)(H_2O)].ClO_4$ (**11**)

Salicylaldehyde (12.1 mg, 0.1 mmol) and 2-aminomethylpyridine (10.8 mg, 0.1 mmol) were dissolved in MeOH (10 mL). The mixture was stirred for 10 min to give a yellow solution, which was added to a stirred aqueous solution (5 mL) of $Cu(ClO_4)_2\cdot 7H_2O$ (38.9 mg, 0.1 mmol). The mixture was stirred for another 10 min at room temperature and then filtered. The filtrate was kept in air for 9 days, forming blue block-shaped crystals of **11**. The crystals were isolated, washed three times with MeOH and dried in a vacuum desiccator containing anhydrous $CaCl_2$. Yield: 59.8%. Analysis: Calcd. for $C_{13}H_{13}ClCuN_2O_6$: C, 39.8; H, 3.3; N, 7.1%. Found: C, 39.9; H, 3.4; N, 7.3%.

The final product yields were calculated with respect to the amount of Schiff base ligands used.

5.3. Crystal structure determination

Diffraction intensities for the eleven complexes were collected at 298(2) K using a Bruker SMART CCD area detector with Mo Kα radiation ($\lambda = 0.71073$ Å). The collected data were reduced using the SAINT program [22], and empirical absorption corrections were performed using the SADABS program [23], the structures were solved by direct methods and refined against F^2 by full-matrix least-squares methods using the SHELXTL program [24]. All of the non-hydrogen atoms were refined anisotropically. The atoms H2A and H2B of the water molecules of **11** were located in a difference Fourier map and refined isotropically, with the O–H and H···H distances restrained to 0.90(1) and 1.47(2) Å, respectively. All other hydrogen atoms were placed in geometrically ideal positions and constrained to ride on their parent atoms. The crystallographic data for the 11 complexes are summarized in Table 2 and Table 3. Selected bond lengths and angles are given in Table 4. Crystallographic data for **1**–**11** have been deposited with the Cambridge Crystallographic Data Center.

5.4. Measurment of XO inhibitory activities

The XO activities with xanthine as the substrate were measured spectrophotometrically, based on the procedure reported by Kong et al. [25], with modification. The activity of xanthine oxidase is measured by uric acid formation monitored at 295 nm. The assay was performed in a final volume of 1 mL 50 mM K_2HPO_4 pH 7.8 in quartz cuvette. The reaction mixture contains 200 μL of 84.8 μg/mL xanthine in 50 mM K_2HPO_4, 50 μL of the various concentrations tested compounds. The reaction is started by addition of 66 μL 37.7 mU/mL xanthine oxidase. The reaction is monitored for 6 min at 295 nm and the product is expressed as μmol uric acid per minute. The reaction kinetics were linear during these 6 min of monitoring.

Acknowledgments

The work was financed by grant (Project 30672516) from National Natural Science Foundation of China.

References

[1] M. Tümer, H. Köksal, M.K. Şener, S. Serin, Trans. Met. Chem. 24 (1999) 414–420.
[2] A.A. Bekhit, O.A. El-Sayed, T.A.K. Al-Allaf, H.Y. Aboul-Enein, M. Kunhi, S.M. Pulicat, K. Al-Hussain, F. Al-Khodairy, J. Arif, Eur. J. Med. Chem. 39 (2004) 499–505.
[3] A. Golcu, M. Tumer, H. Demirelli, R.A. Wheatley, Inorg. Chim. Acta 358 (2005) 1785–1797.
[4] K. Singh, M.S. Barwa, P. Tyagi, Eur. J. Med. Chem. 41 (2006) 147–153.
[5] J. Chakraborty, R.N. Patel, J. Indian Chem. Soc. 73 (1996) 191–193.
[6] D.J. Hearse, A.S. Manning, J. Downey, D.M. Yellon (Suppl. 548), Acta Physiol. Scand. (1986) 65–78.
[7] P.H. Chan, J.W. Schimidley, R.A. Fishman, S.M. Longar, Neurology 34 (1984) 315–320.
[8] H.S.D. Naeff, M.C.R. Franssen, H.C. Van der Plas, Recl. Trav. Pays-Bas. 110 (1991) 139–150.
[9] R.K. Robins, G.R. Revankar, D.E. O'Brien, R.H. Springer, T. Novinson, A. Albert, K. Senga, J.P. Miller, D.G. Streeter, J. Heterocycl. Chem. 22 (1985) 601–634.
[10] A. Haberland, H. Luther, I. Schinker, Agents Actions 32 (1991) 96–97.
[11] Z.-L. You, D.-H. Shi, H.-L. Zhu, Inorg. Chem. Commun. 9 (2006) 642–644.
[12] M.S. Mondal, S. Mitra, J. Inorg. Biochem. 62 (1996) 271–279.
[13] W.J. Geary, Coord. Chem. Rev. 7 (1971) 81–122.
[14] Z.-L. You, H.-L. Zhu, Z. Anorg. Allg. Chem. 630 (2004) 2754–2760.
[15] K.R. Reddy, M.V. Rajasekharan, J.P. Tuchagues, Inorg. Chem. 37 (1998) 5978–5982.
[16] H.-L. Zhu, Q.-F. Zeng, D.-S. Xia, X.-Y. Liu, D.-Q. Wang, Acta Crystallogr. E59 (2003) m777–m779.
[17] Z.-L. You, Y. Qu, W.-S. Liu, M.-Y. Tan, H.-L. Zhu, Acta Crystallogr. E59 (2003) m1038–m1040.
[18] Z.-L. You, H.-L. Zhu, Acta Crystallogr. C60 (2004) m445–m446.
[19] Z.-L. You, Z.-D. Xiong, H.-L. Zhu, Acta Crystallogr. E60 (2004) m1114–m1116.
[20] Z.-L. You, B. Chen, H.-L. Zhu, W.-S. Liu, Acta Crystallogr. E60 (2004) m884–m886.
[21] S.-Y. Li, Z.-L. You, B. Chen, Y.-S. Lin, Z.-D. Xiong, H.-L. Zhu, Acta Crystallogr. E60 (2004) m999–m1001.
[22] Bruker, SMART (version 5.628) and SAINT (version 6.02), Bruker AXS Inc., Madison, Wisconsin, USA, 1998.
[23] G.M. Sheldrick, SADABS, Program for Empirical Absorption Correction of Area Detector, University of Göttingen, Germany, 1996.
[24] G.M. Sheldrick, SHELXTL V5.1, Software Reference Manual, Bruker AXS, Inc., Madison, Wisconsin, USA, 1997.
[25] L.-D. Kong, Y. Zhang, X. Pan, R.-X. Tan, C.H.K. Cheng, Cell. Mol. Life Sci. 57 (2002) 500–505.